

Power Quality Improvement of Grid Interactive DFIG based WECS with Fractional Order Sliding Mode Controller

Banda.Sandeep¹, Dr.T. Anil kumar², Dr.C. Nagamani³, Dr.G. Venu Madhav⁴

¹PG Scholar, Department of Electrical and Electronics Engineering, Anurag Group of Institutions (Anurag University), Venkatapur, Ghatkesar, Medchal malkajgiri District, Telangana, India 500088

^{2,3,4}Professor, Department of Electrical and Electronics Engineering, Anurag University, Venkatapur, Ghatkesar, Medchal Malkajgiri District, Telangana, India 500088

Abstract: The primary objective of this project is power quality improvement of Wind energy conversion schemes based on grid cooperating double fed induction generators with FOSMC control strategy. A doubly fed induction generator founded WECS system that interacts with the grid shares reactive power between two converters in this article. In this project Rotor side and Grid side Modular Multilevel Converters (MMC) are used for reduction of harmonics in the waveform. In order to limit the amount of copper losses in the rotor winding, Rotor Side Modular Multilevel Converter (RS-MMC) management of the DFIG is designed and to share reactive power at lower wind speeds. It is, however, designed to keep stator terminals operating at unity power factor at rated wind speeds while still extracting the rated power without exceeding its rating. Reactive power distribution also reduces copper loss in rotor windings, as seen in the example. Aside from that, the GSMMC (Grid-Side Modular Multilevel Converter) control provides grid-side and load-coupled DFIG and load with reactive power support for power flow regulation. The GSC-MMC control is devised to adjust for load imbalance and harmonics. Battery Energy Storage System (BESS) coupled to DC link of Back-to-Back MMCs ensures that the regulates the power flow of grid under fluctuations in wind speed. Simulations are run in MATLAB to see how the system performs with varied grid reference active power, changing wind speed, reactive power sharing, and unstable nonlinear loads. The design of Fractional Order Sliding Mode Controller (FOSMC) at GS-MCC, RS-MMC to mitigate the powerquality issues such as THD of grid integrated WECS.

Keywords: Power quality, doubly fed induction generator (DFIG) Rotor side modular multilevel converter (RS-MMC), Grid side modular multilevel converter (GS-MMC), fractional order sliding mode controller (FOSMC)

I.INTRODUCTION

The rise in population and industrialization has led to an increase in energy consumption. Although coal, oil, and gas are the most common sources of conventional energy, these resources are finite in scope. In order to meet the world's growing demand for energy in the future, we must now turn to renewable resources [1]. The fact that this renewable resource is non-polluting and limitless in nature are other major advantages [2]. The cost of wind power is now equivalent to that of conventional power plants because of technological developments. As a result, of all the renewable energy options, wind power is the most popular [3]. Squirrel cage induction generators and capacitor banks were initially utilized in fixed-speed wind turbines. Because of their simplicity and low cost, the majority of wind turbines are fixed-speed [4]. The machine can run at a variety of speeds thanks to contemporary power electronic converters [5]. It's therefore possible to increase the amount of renewable energy generated by these variable-speed turbines DFIGs are the most popular variable-speed wind turbines because of their inexpensive cost. Additional benefits include advanced energy output, lower converter rating and improved generator usage [8]. For the weak grid, these DFIGs give excellent damping performance. Using the decoupled vector control technique described in [10, 11], it is possible to independently regulate the active and reactive power. The vector control of such a system is often implemented in a synchronously rotating reference frame oriented in either the voltage or flux axis. In this study, a voltage-oriented reference frame is used to achieve RSC control. There are grid code regulations for wind farm grid connection and operation in [12]. In [13] compares the responsiveness to grid disturbances of the DFIG-based wind energy conversion system (WECS) with that of the fixed speed WECS.

While the GSC is responsible for maintaining DC link voltage, RSC typically fulfils DFIG's reactive power requirements for magnetization. The reactive power can be shared across two converters, thanks to control mechanisms proposed by some researchers. Reactive power distribution between converters in a DFIG has been the subject of several control techniques described by Kahiki et al. However, there is no explanation of how to supply the DFIG itself with reactive power. Reactive power sharing is not taken into consideration by the authors, which results in additional power loss. Despite this, the writers haven't talked about the loss of power in the rotor and stator windings. In addition, no discussion of hardware implementation of control mechanisms is included. As wind speed fluctuates, so does the amount of electricity generate by DFIG. When power is generated and sent to the grid, problems arise, especially if the grid is poor, as it is in rural areas. There are two ways to regulate power flow in the grid using the wind energy conversion system: with and without energy storage. Batteries, supercapacitors, flywheels, fuel cells, and superconducting magnetic energy storage (SMES) are all forms of energy storage. Non-energy-storage features include inertia and

pitch angle control, as well as DC link voltage adjustment. There's a lot of information out there about how to regulate power flow on the grid in. Using a variable frequency transformer, Wang et al. [14] have been power oscillations in the grid have been eliminated.

Furthermore, there is no evidence that it works. Using an optimized power point tracking technique, Ochoa et al. [15] the subject of power grid stability was discussed. If you've ever wondered how to get the most out of your battery, you've come to the right place. This means that the WECS does not run at maximum power point tracking (MPPT) in order to level out the grid's output. Furthermore, when the generation is larger than or equal to the grid reference power, it is desirable to modify the MPPT for power smoothing. When the maximum generation is less than the reference grid power, this method cannot be relied upon because there is no other source of power to balance it. Furthermore, there is no mention of how this technology could be implemented on hardware. Using a superconducting magnetic energy storage device, the authors in [13] show how to remove grid power fluctuations. The control circuits and the entire system grow more complicated, though, using this way. The system's theoretical analysis is not validated by the test findings, either. The smoothing of grid electricity by BES is explored in [14]. Based on wind patterns at a specific location, the scientists have created a BES that can store energy. Disturbances can cause changes in both active and reactive power flow, however this hasn't been addressed by authors. [15], [16] describe some of the MPPT strategies that can be used to obtain maximum power from a wind turbine. One of the two modular multilevel converters used in this work is called DFIG and is used in conjunction with the grid-interactive WECS.GS-MMC and RS-MMC. The main intention of MMC is reduce the THD in output voltage and improving the power quality.

Nonlinear systems can benefit from the sliding mode control (SMC) strategy, which is a reliable and high-frequency method. SMC's advantages include its high level of robustness, rapid convergence speed, and ease of implementation [13]-[16]. Nevertheless, SMC's principal downside is the chattering issue, which may affect its overall performance when operating some high-frequency harmonics-vulnerable systems [17]. To address the issue, countermeasures were presented to reduce the level of chattering in robot control, an exponential reaching law (ERL) has been proposed [18]. [19] proposes Integer order calculus underpins the aforementioned SMC systems, which make use of differentiators or integrators of integer order. It has recently been hypothesized that the concept of fractional order sliding mode control (FOSMC) is based on fractional order calculus (FOC).

Control elements of DFIG are the focus of this research.

The RS-MMC control supplies about 60 percent of the machine's reactive power from the rotor in order to minimize copper losses.

An example is used to demonstrate reactive power sharing between RS-MMC and GS-MMC.

Through the use of unit templates, the GS-MMC is managed by indirect vector control, which ensures smooth grid operation.

Regardless of the wind speed, grid power flow can be regulated by connecting the BES to the DC link between two modular multilevel voltage source converters.

II. BLOCK DIAGRAM MODEL OF WIND ENERGY CONVERSION SYSTEM

Grid-interactive WECS, as indicated in Fig. 1, it includes a DFIG-based WECS of 10 kW capacity, a BES, and the utility grid. A DC link connects the BES directly to the network. There is an LCB (line circuit breaker) that connects the stator of DFIG to the grid and also connects the entire system to the grid. The approach described here is used to develop wind-driven DFIGs, BESs, Δ/Y transformers (T/Fs), DC link capacitors, interface inductors, and ripple filters.

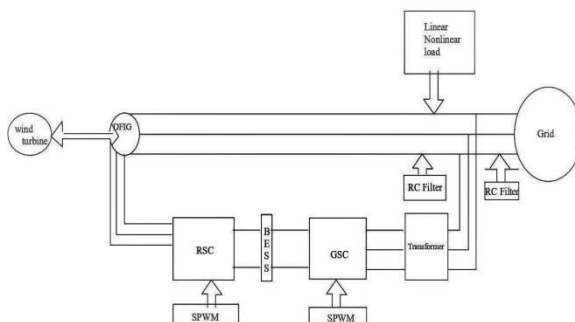


Figure.1 Wind energy conversion system with BES grid-interactive

III. WIND ENERGY CONVERSION SYSTEM WITH FOSMC

There is a diagram of the FOSMC based DFIG in Fig.2 that shows the WECS, BES, utility grid, and the modular multilevel converters (9level MMCs) RS and GS, as well as the DFIG based WECS of 10kW capacity. A DC link connects the BES directly to the network. Design of DFIG, BES, Δ/Y transformer (T/F), interface inductors, and ripple filters. The GS-MMC and RS-MMC are controlled by PWM control technique with FOSMC controller.

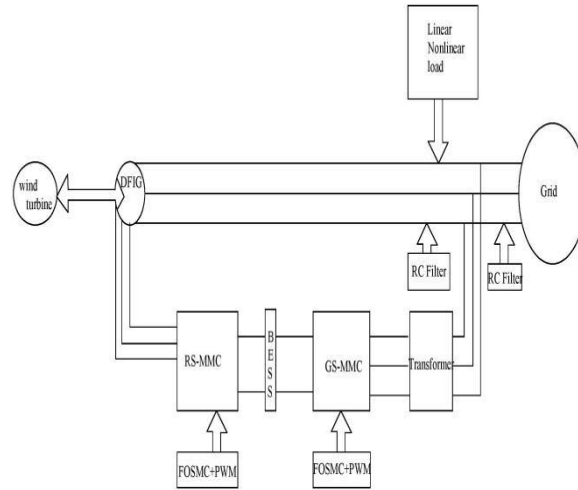


Figure.2 Wind energy conversion system based on FOSMC and interconnected with the BES grid

IV. CONTROL STRATEGY

A) RS-MMC CONTROLLING

RSC control is designed using a flux-based reference frame. Additionally, it serves as an MPPT controller for a wind turbine and a component of the DFIG's magnetizing power. Figure 3 depicts the RSC control.

There are two methods for determining I_{qr}^* : TSR technique is used to calculate the MPPT of wind turbines, and it takes into account measurements of both wind speed (V_w) and rotor rotation speed (r). based on the TSR-MPPT technique, the speed set point,

$$\omega_r^* = \eta \lambda^* V_w / r \quad (1)$$

Where gear ratio, tip-to-gear speed ratio, and turbine radius are referred to as λ^* , η and r . To generate I_{qr}^* , a proportional-integral (PI) speed controller is fed the difference in speed between the reference and real speeds.

$$I_{qr}^*(k) = I_{qr}^*(k-1) + K_{p\omega}(\omega_{err}(k) - \omega_{err}(k-1)) + K_{i\omega}\omega_{err}(k) \quad (2)$$

Speed error $\omega_{err}(k)$ is calculated by comparing the reference and estimated speeds.

$$\omega_{err}(k) = \omega_r^*(k) - \omega_r(k) \quad (3)$$

2) Calculation of I_{dr}^* : DFIG's reference exciting current, I_{dr}^* , is used to make this calculation. The machine's no-load magnetising current, I_{ms0} , is reflected in the value of I_{dr}^* . [19] is the value of I_{ms0} , according to the formula.

$$I_{ms0} = \frac{\sqrt{2}V_L}{\sqrt{3}X_m} \quad (4)$$

where X_m is the machine's magnetizing reactance and V_L is the voltage at the line applied to machine's terminal with the 80 percent confidence interval for wind speeds at the 30 m altitude, the WECS power output is expected to be within 0.6% of that time. The winding loss is increased because the Rotor windings works at a lesser voltage, keeps the I_{dr}^* as I_{ms0} . Since the RS-MMC control supplies 60 percent of no-load magnetizing current, the GSC is responsible for the remaining 40%. This is how we arrive at I_{dr}^* :

$$I_{dr}^* = k_R \times I_{ms0} \quad (5)$$

Here, k_R is equal to 0.6. However, when wind speeds approach the specified value, the RSC supplies all of the DFIG's reactive power needs, allowing the stator to produce its maximum rated power. The stator functions at unity power factor at wind speeds close to the rated value. Switching logic is used to generate the I_{dr}^* component of rotor current. RS-MMC and GSC-MMC share reactive power, as well as the advantages of doing so, in the following section, with several examples.

Feeding the signal created by the FOSMC and delivered to the pulse width modulation (PWM) generator generates the RS-MMC switching signals. Fig. 3 depicts the set up.

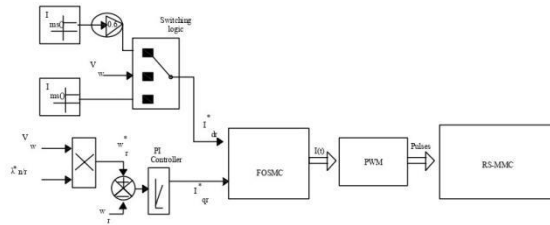


Fig.3. Control of RS-MMC.

B) GS-MMC CONTROLLING

GS-MMC controls the battery's power output based on its SOC. GS-MMC employs the subsidiary current control technique as indicated in Fig.4.

Unit templates for in-phase components can be generated using phase voltages.

$$u_{ap} = \frac{V_{an}}{V_g}, u_{bp} = \frac{V_{bn}}{V_g}, u_{cp} = \frac{V_{cn}}{V_g} \quad (6)$$

As determined by multiplying by V_g to get the peak phase voltage at the PCC

$$V_g = \{2(V_{an}^2 + V_{bn}^2 + V_{cn}^2)/3\}^{1/2} \quad (7)$$

Additionally, the PCC's instantaneous phase voltages are represented by V_{an} , V_{bn} and V_{cn} . It is seen in Fig.4 that the generated dq signals are sent to FOSMC and compared to the carrier signal in the PWM generator. The pulse width modulation (PWM) generator generates the GS-MMC switching signals.

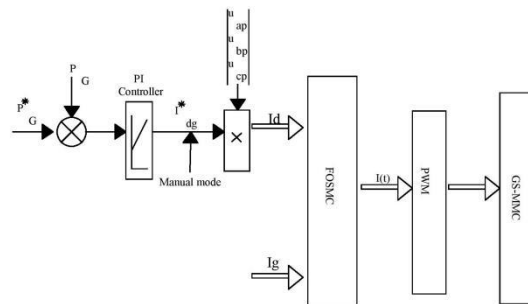


Fig.4. Control of GS-MMC.

V.CONTROL STRUCTURE OF FOSMC

The below figure 4.1 shows the fractional order sliding mode control algorithm for controlling the RS-MMC and MS-MMC.

The direct and quadrature components are generated by taking the feedback signals voltage (RS-MMC) and current (GS-MMC). The direct and quadrature signals passed through the fractional order block and it is given by equivalent voltage for (RS-MMC) and current for (GS-MMC) as shown in figure 4.1. By using pulse width modulation technique switching pulses to the converters are generated i.e., In which the output equivalent signal and the carrier waveform are both measured and compared After that, the converter switches receive the generated pulses.

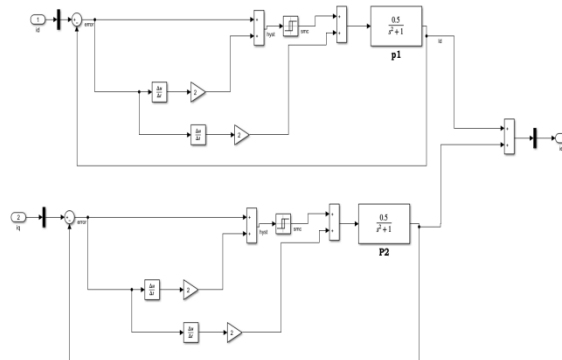


Fig 4.1 FOSMC control

VI.SIMULATION RESULTS

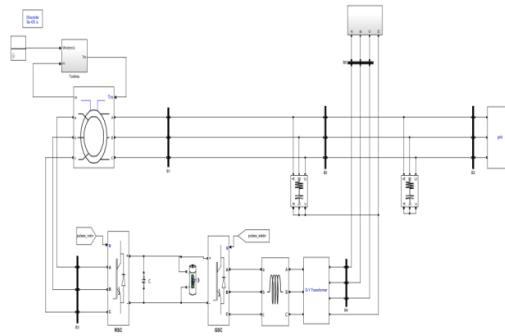


FIG .5 MATLAB/SIMULINK circuit diagram of the proposed system

A) EXISTING RESULTS

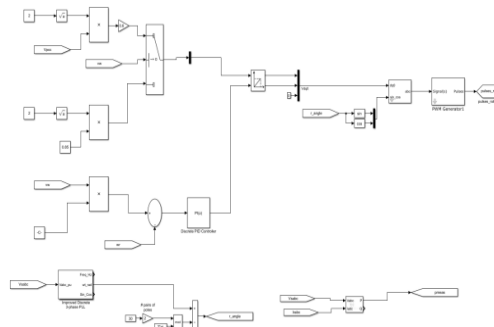


Fig .6 Implementation of RSC

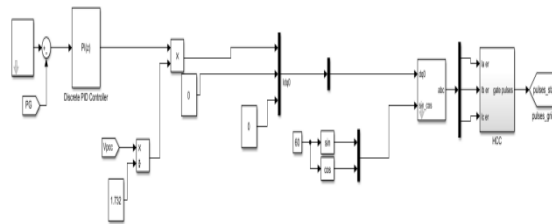


Fig.7 Implementation of GSC

A. The System's Performance During Incremental Changes in Active Reference power

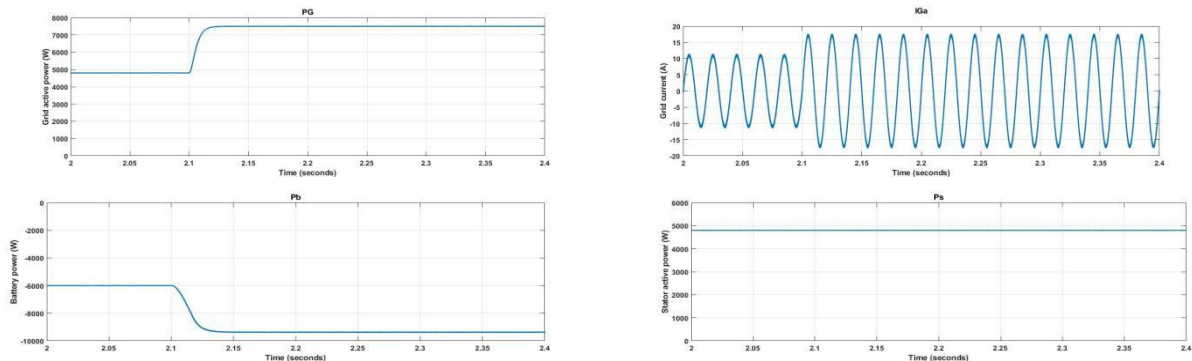


Fig.8 (PG) Active Power at Grid, (IGa) Current at the Grid, (Pb) Power at Battery, Active Power at the Stator (Ps)

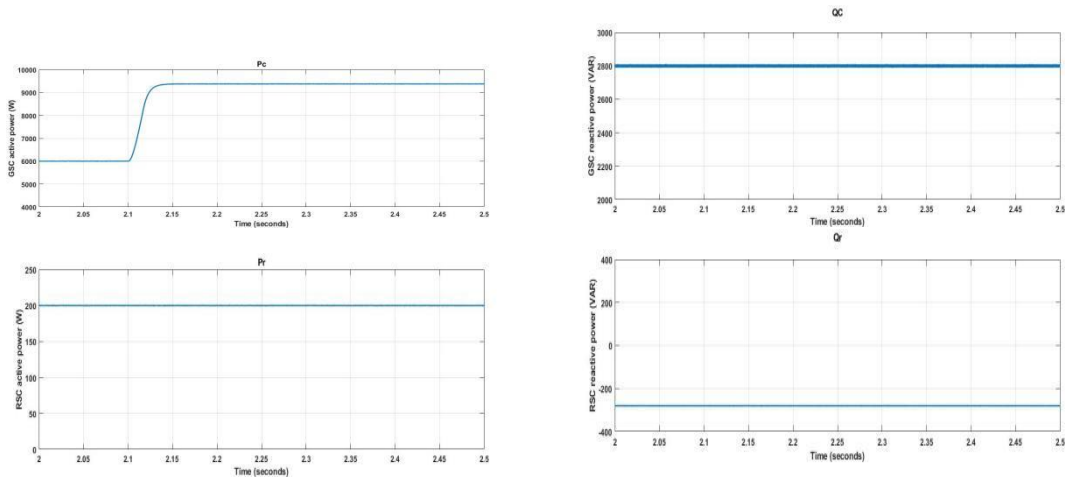


Fig.9. Active Power at Grid Side Converter (PC), Reactive Power at Grid Side Converter (QC), Active Power at Rotor Side Converter (Pr) and Reactive Power at Rotor Side Converter (Qr)

B. System Performance with Varying Wind Speeds

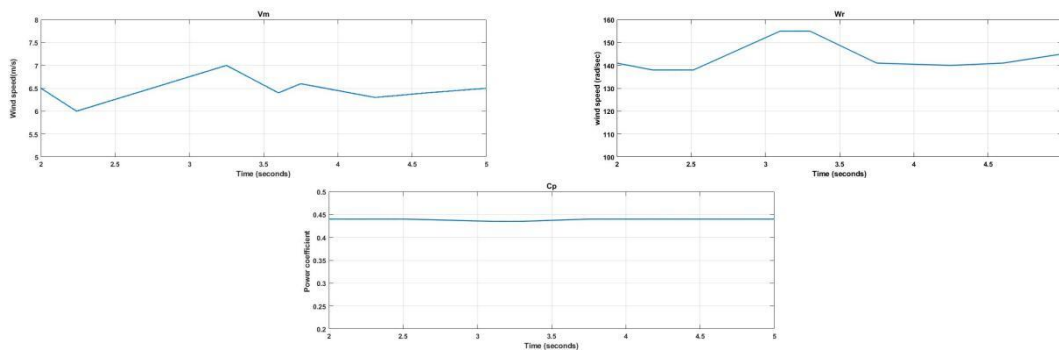


Fig.10 (a) Speed of the Wind (V_w), Speed of the Rotor (ω_r), Turbine Power Coefficient (C_p)

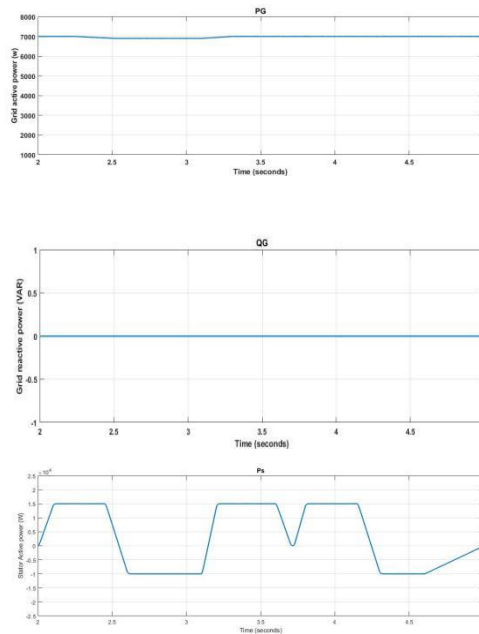


Fig.11 Active Power at the Grid (PG), Reactive Power at the Grid (QG), Active Power at the Stator (Ps)

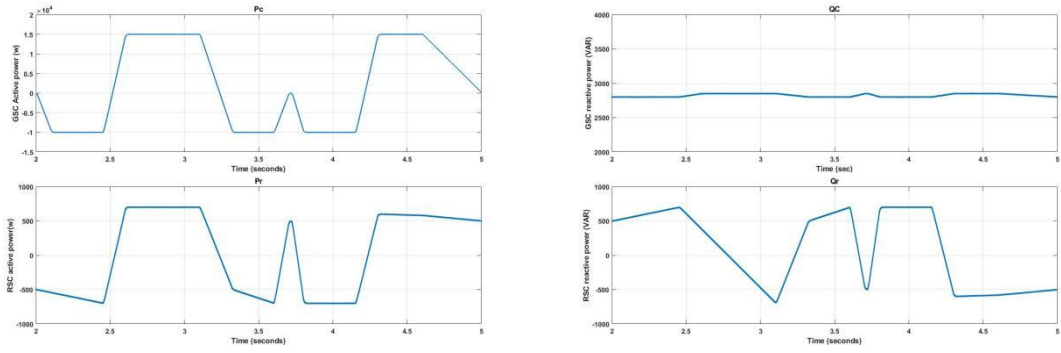


Fig.12 Active Power at Grid Side Converter (PC), Reactive Power at Grid Side Converter (QC), Active Power at Rotor Side Converter (Pr) and Reactive power Rotor Side Converter (Qr)

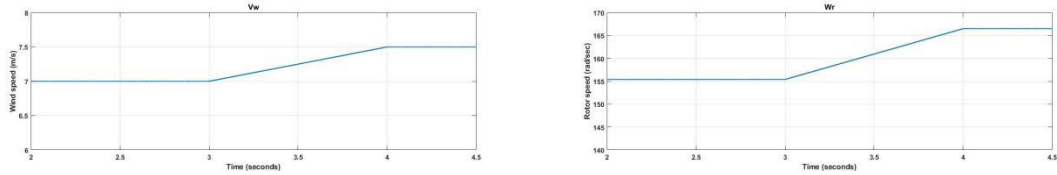


Fig.13 Wind Speed (V_w) and Rotor Speed (ω_r)

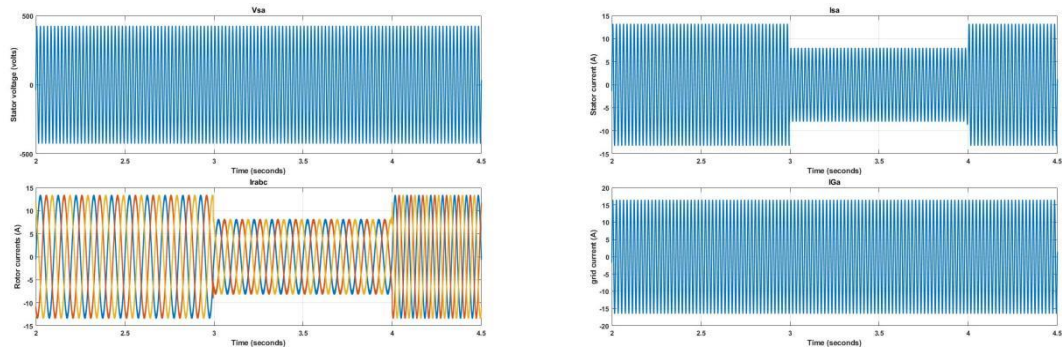


Fig.14 Stator Voltage (v_{sa}), Stator Current (i_{sa}), Rotor Currents (i_{rabc}), Grid Current (i_{Ga})

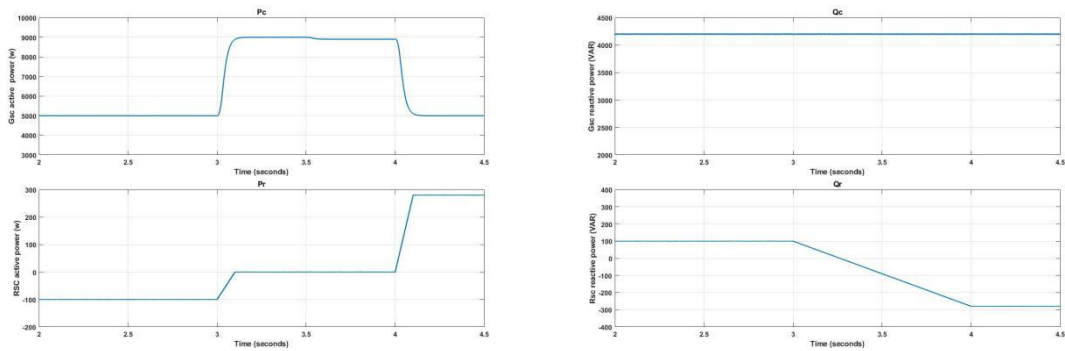


Fig.15 Active Power at Grid Side Converter (PC), Reactive Power at Grid Side Converter (QC), Active Power at Rotor Side Converter (Pr) and Reactive Power at Rotor Side Converter (Qr)

C. Performance of the System During Reactive Power At load changes, sharing among Rotor side converter and Grid side converter

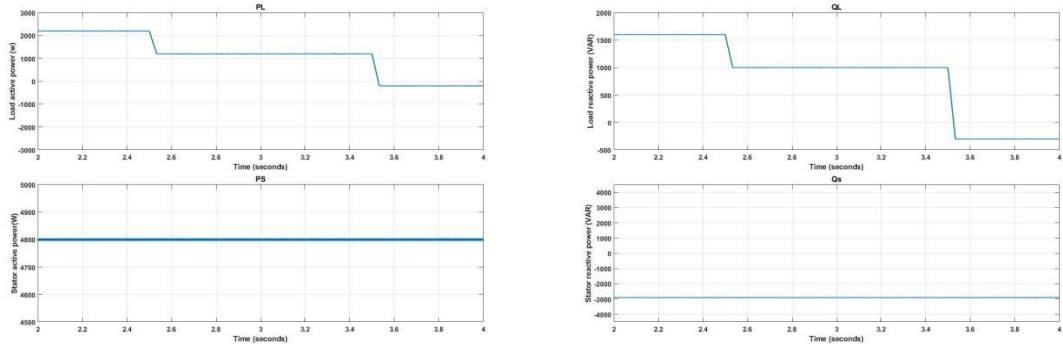


Fig 16.1 Load Power (PL), Reactive Power atLoad (QL), Active Power at Stator (Ps), Reactive Power at Stator (Qs)

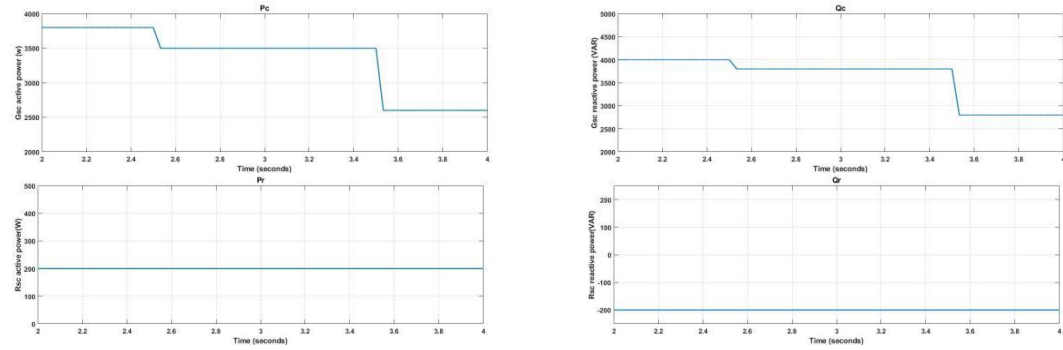


Fig. 17 Active Power at Grid Side Converter (PC), Reactive Power at Grid Side Converter (QC), Active Power at Rotor Side Converter (Pr) and Reactive Power at Rotor Side Converter (Qr)

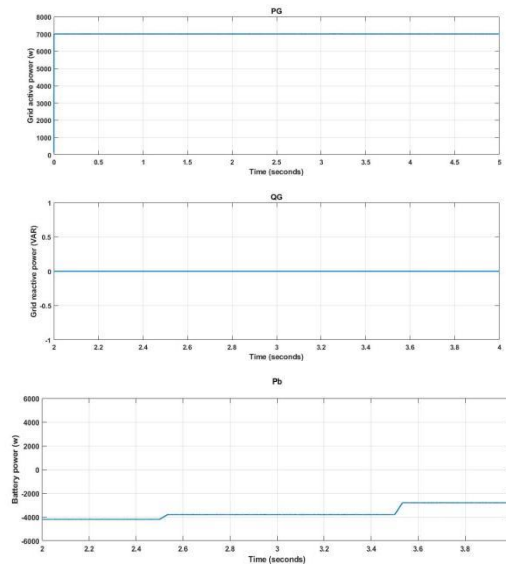
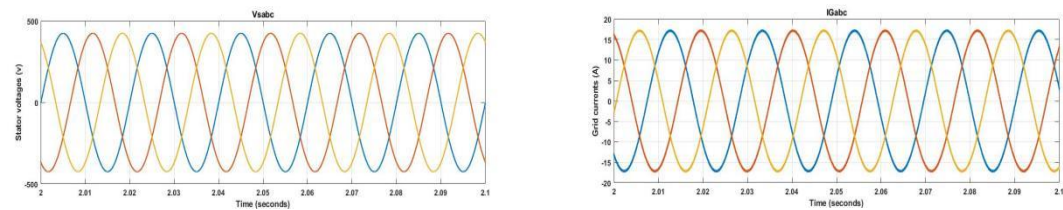


Fig 18 Active Power at Grid (PG), Reactive Power at Grid (QG), Power at the Batter (Pb)

D. Unbalanced Nonlinear Loads Affecting System Performance



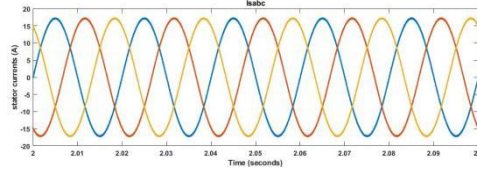


Fig.19 Voltages at the Stator (V_{sabc}), Currents at the Grid (I_{Gabc}), Currents at the Stator (I_{sabc})

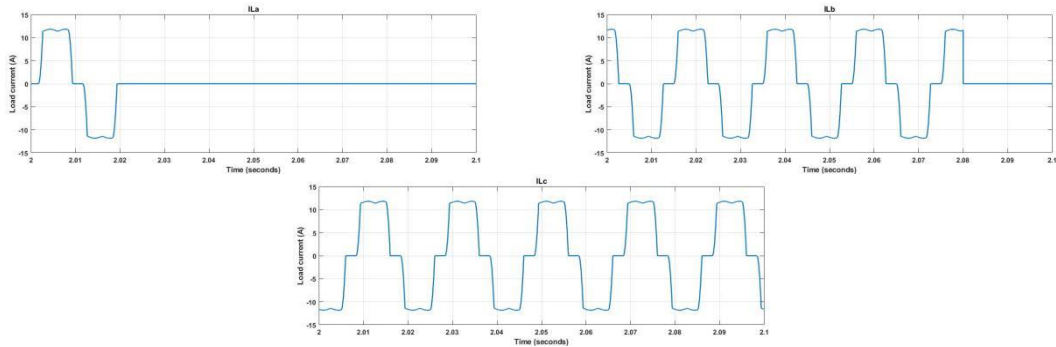


Fig.20 Load Currents (i_{La} , i_{Lb} , i_{Lc})

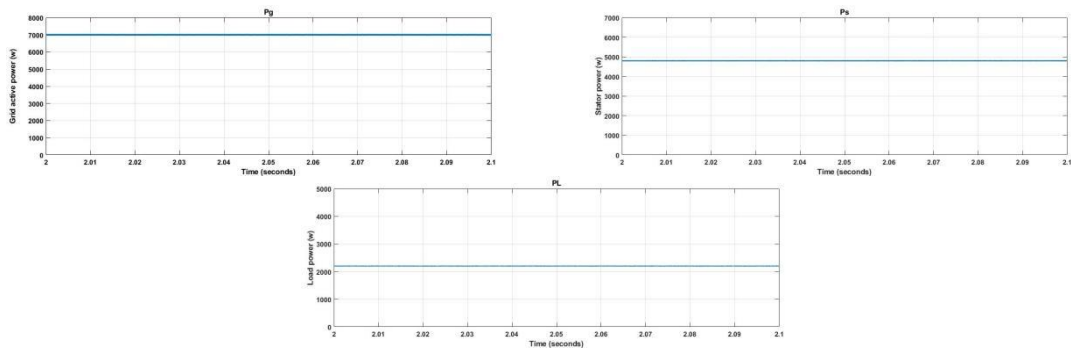


Fig.21 Active Power at the Grid (P_G), Power at Stator (P_s), and Power at the Load (P_L)

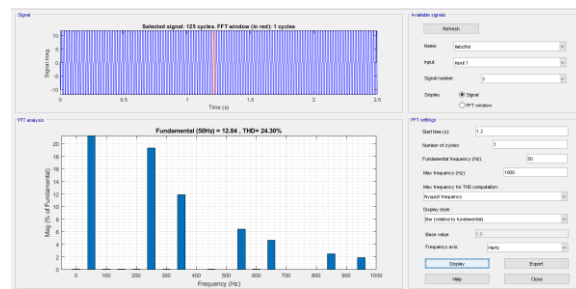


Fig.22. Load Current THD 24.30%

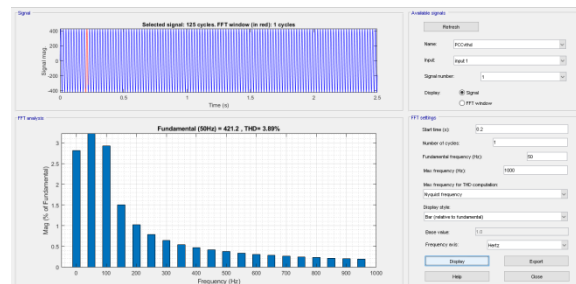


Fig 23.PCC Voltage THD 3.89%

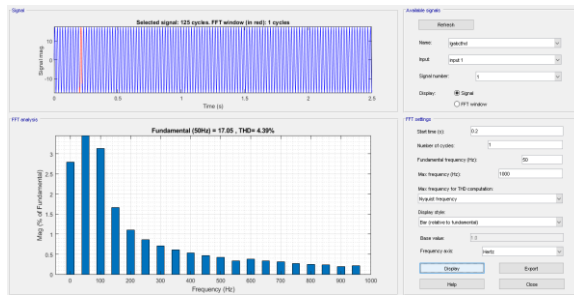


Fig.24. Grid Current THD 4.39%

B) EXTENSION RESULTS

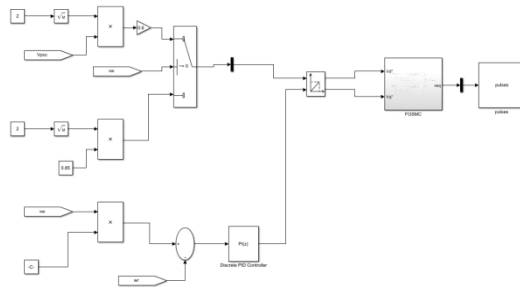


Fig.25 RS-MMC control subsystem

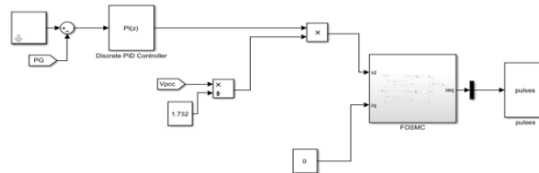


Fig.26 GS-MMC control subsystem

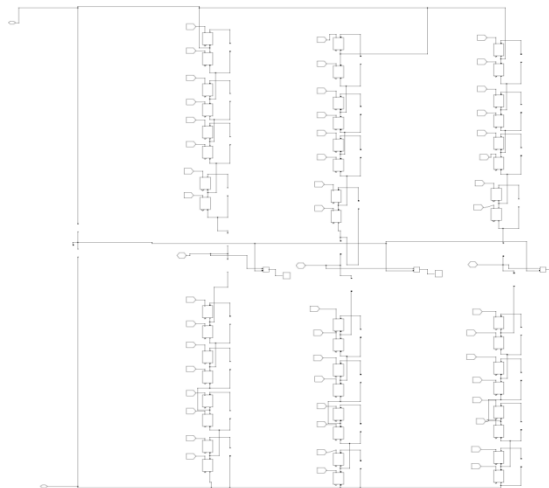


Fig.27 MMC sub system

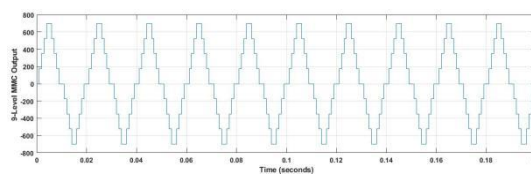


Fig.28 MMC Nine level output voltage

A. The System's Performance During Incremental Changes in Active Reference Power

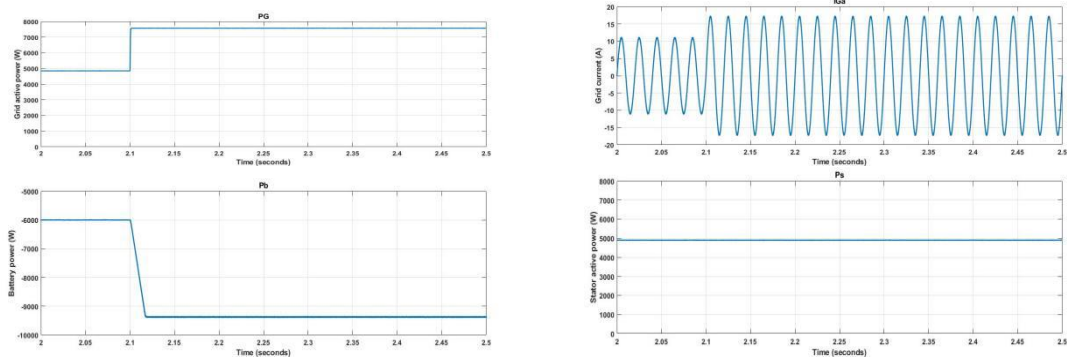


Fig.29 Active Power at the Grid (PG), Current at the Grid (i_{Ga}), Power at Battery (Pb), Active Power at the Stator (Ps)

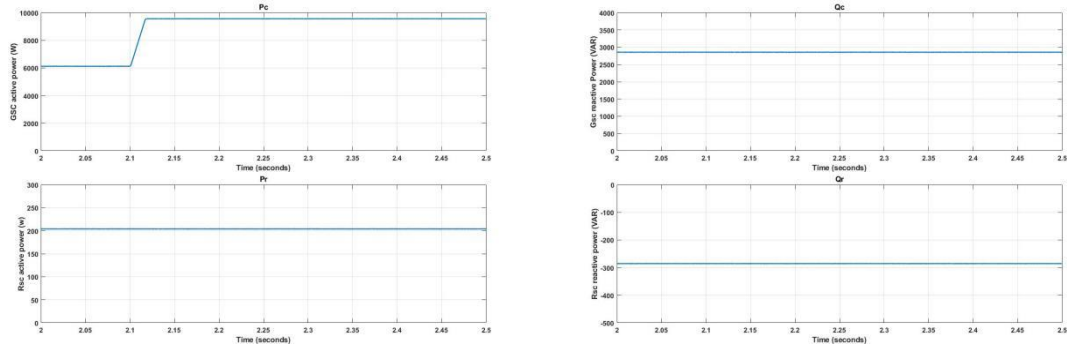


Fig.30 Active Power at Grid Side MMC (PC), Reactive Power at Grid Side MMC(QC), Active Power at Rotor Side MMC (Pr) and Reactive Power at Rotor Side MMC (Qr)

B. System Performance with Varying Wind Speeds

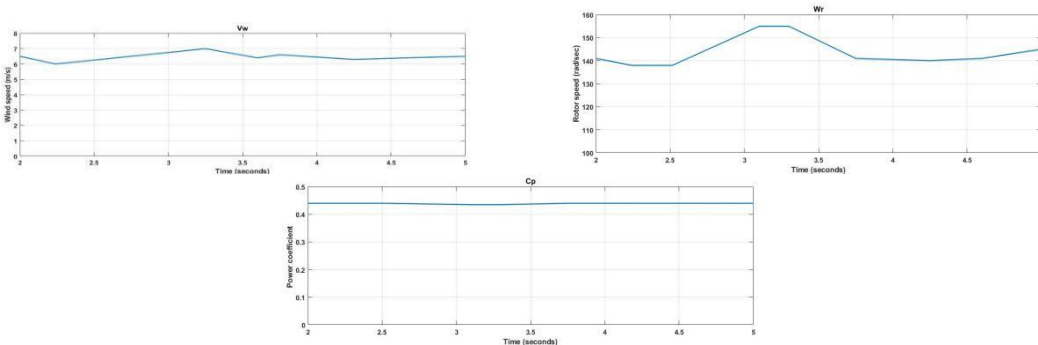


Fig.31 (a) Speed of Wind (V_w), Speed of the Rotor (ω_r), Turbine Power Coefficient (C_p)

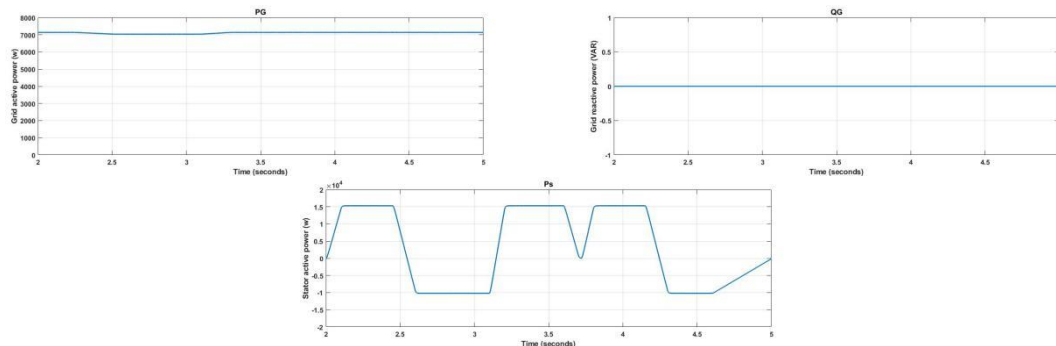


Fig.32 Active Power at the Grid (PG), Reactive Power at the Grid (QG), Active Power at the Stator (Ps)

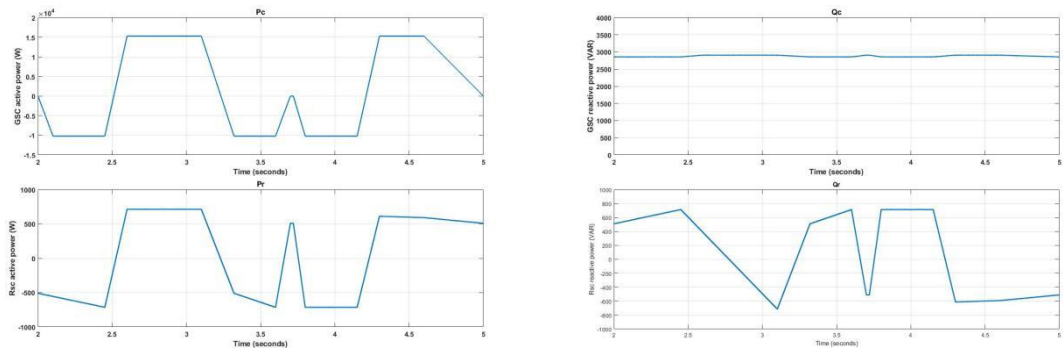


Fig.33 Active Power at Grid Side MMC (Pc), Reactive Power at Grid Side MMC(Qc), Active Power at Rotor Side MMC (Pr) and Reactive Power at Rotor Side MMC (Qr)

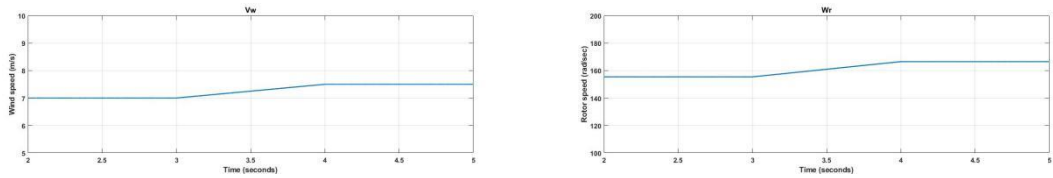


Fig.34 Wind Speed (Vw) and Rotor Speed (ω_r)

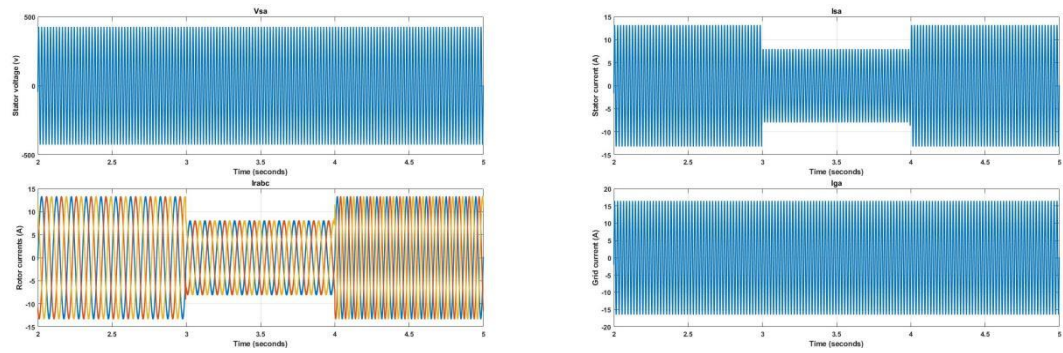


Fig.35 Stator Voltage (vsa), Stator Current (isa), Rotor Currents (irabc), Grid Current (iGa),

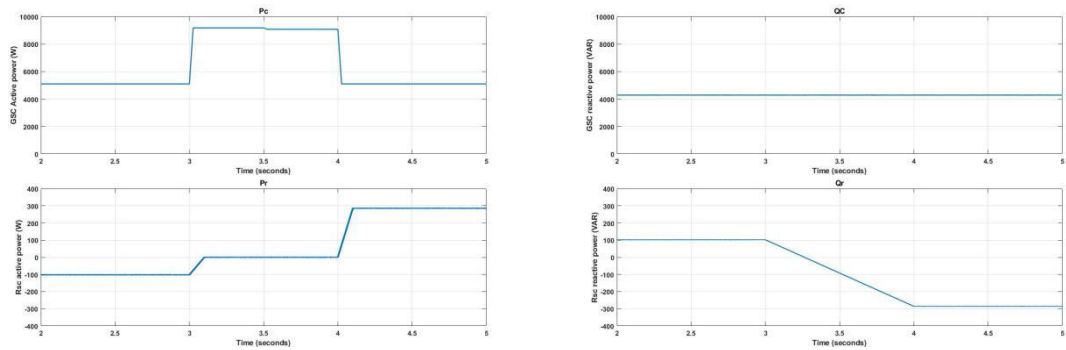
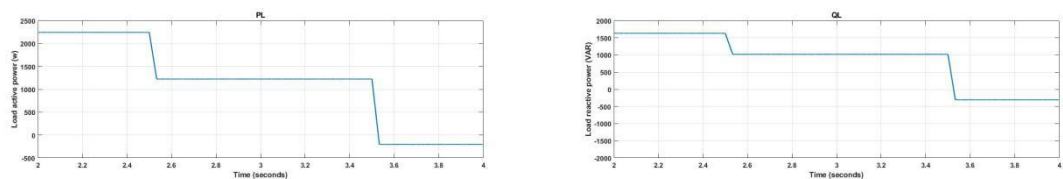


Fig.36 Active Power at Grid Side MMC (Pc), Reactive Power at Grid Side MMC(Qc), Active Power at Rotor Side MMC (Pr) and Reactive Power at Rotor Side MMC (Qr)

C. Performance of the System During Reactive Power At load changes, sharing among Rotor side converter and Grid side converter



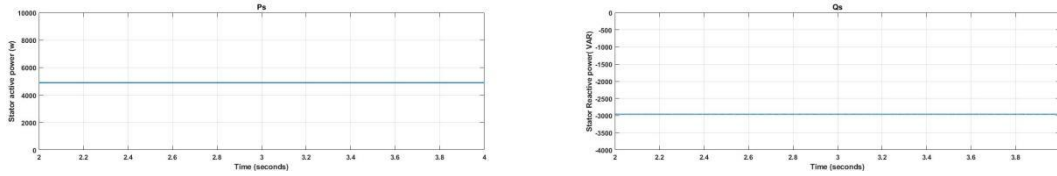


Fig.37 Active Power at the Load (PL), Reactive Power at the Load (QL), Active Power at Stator (Ps), Reactive Power at Stator (Qs)

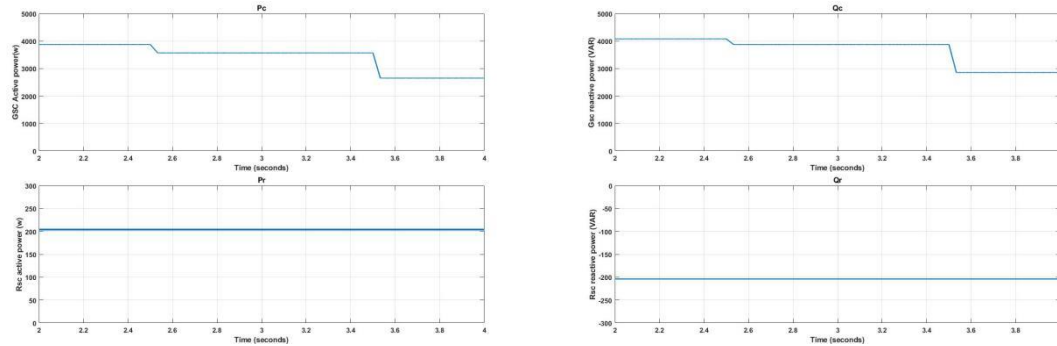


Fig.38 Active Power at Grid Side MMC (PC), Reactive Power at Grid Side MMC(QC), Active Power at Rotor Side MMC (Pr) and Reactive Power at Rotor Side MMC (Qr)

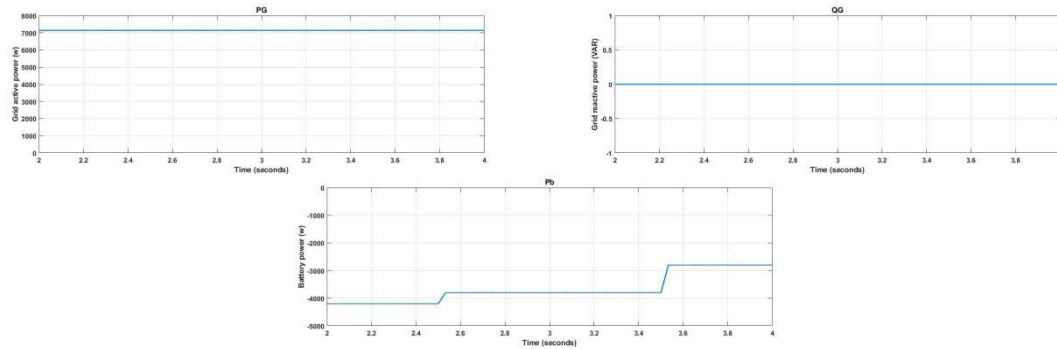


Fig. 39 Active Power at the Grid (PG), Reactive Power at the Grid (QG), Power at Battery (Pb)

D. Unbalanced Nonlinear Loads Affecting System Performance

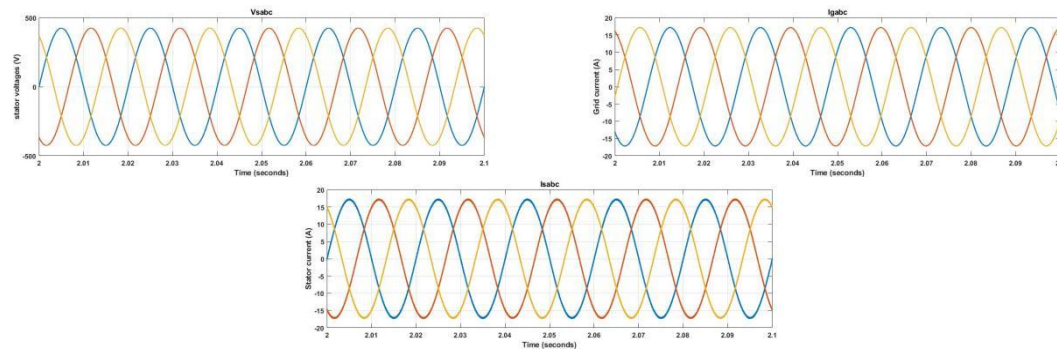


Fig 40 Voltages at the Stator (Vsabc), Currents at the Grid (IGabc), Currents at the Stator (Isabc),

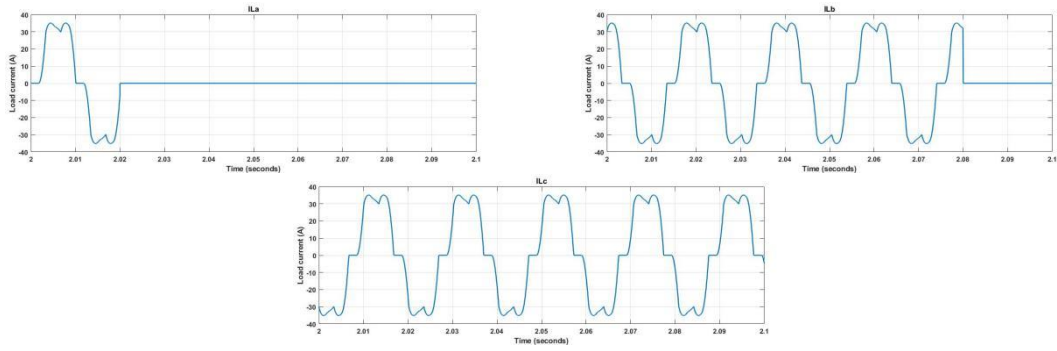


Fig.41 Load Currents (ILa, ILb, ILc),

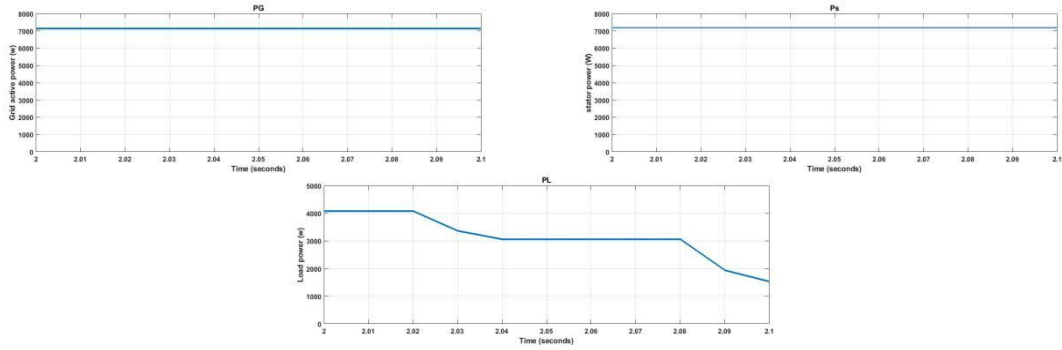


Fig.42 Active Power at Grid (PG), Power at Stator (Ps), and Power at Load (PL).

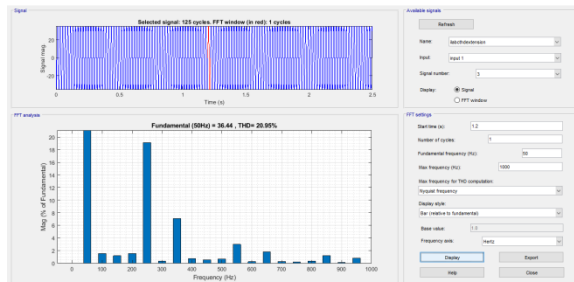


Fig .43 Load Current THD 20.95%

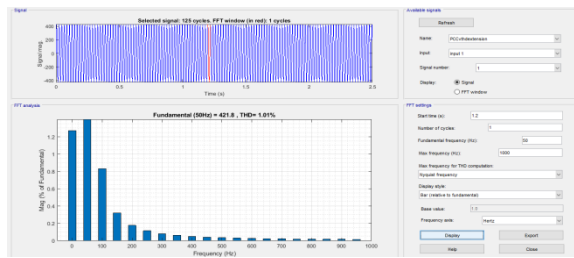


Fig.44 PCC Voltage THD 1.01%

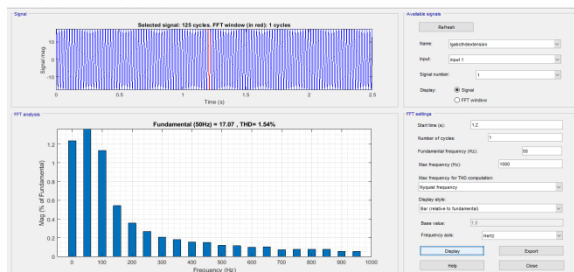


Fig.45 Grid Current THD 1.54%

Comparison table :-

	Existing system	Proposed system
Grid Current THD	4.39%	1.54%
PCC Voltage THD	3.89%	1.01%
Load Current THD	24.30%	20.95%

CONCLUSION

This paper proposes a power quality improvement of Wind energy conversion systems based on grid cooperating double fed induction generators with Fractional order sliding mode controller (FOSMC). At lower wind speeds, the distribution of reactive power among converters results in a loss of power, rotor winding copper losses have been significantly reduced. The reduction or increase in the converter's losses is also minimally affected by the use of reactive power sharing. And in the proposed system modular multilevel converters (MMCs) used for reducing the harmonics in rotor side and also grid side. Furthermore, there is indication that RS-MMC control can distribute reactive power at low wind speeds, preserve unity power factor at the turbine's maximum speed, and collect maximum power from the wind turbine at that speed. The GS-MMC control has also been proven to be effective in regulating power flow, compensating the DFIG stator and load for reactive power, compensating the harmonics and unbalance of the loads, and attaining power flow regulation. An acceptable performance attribute of BESS is that it maintains a steady grid power flow regardless of wind speed change. FOSMC's better performance over conventional control theory was completely validated through simulations. Final simulation tests confirmed the suggested FOSMC method's effectiveness and superior performance.

REFERENCES

- [1] D. M. Tagare, et.al., *Electric Power Generation the Changing Dimensions*. Piscataway, NJ, USA: IEEE Press, 2011.
- [2] G. M. Joselin Herbert, et.al., "A review of technical issues on the development of wind farms," *Renew. Sustain. Energy Rev.*, vol. 32, pp. 619–641, 2014.
- [3] I. Munteanu, et.al., *Optimal Control of Wind Energy Systems Towards a Global Approach*. Berlin, Germany: Springer-Verlag, 2008.
- [4] A. A. B. Mohd Zin, et.al., "An overview on doubly fed induction generators controls and contributions to wind-based electricity generation," *Renew. Sustain. Energy Rev.*, vol. 27, pp. 692–708, Nov. 2013.
- [5] S. S. Murthy, et.al., "A comparative study of fixed speed and variable speed wind energy conversion systems feeding the grid," in *Proc. IEEE Conf. Power Electron. Drive Syst. (PEDS'07)*, Nov. 27–30, 2007, pp. 736–743.
- [6] D. S. Zinger, et.al., "Annualized wind energy improvement using variable speeds," *IEEE Trans. Ind. Appl.*, vol. 33, no. 6, pp. 1444–1447, Nov./Dec. 1997.
- [7] H. Polinder, et.al., "Comparison of direct-drive and geared generator concepts for wind turbines," *IEEE Trans. Energy Convers.*, vol. 21, no. 3, pp. 725–733, Sep. 2006.
- [8] R. Datta, et.al., "Variable-speed wind power generation using doubly fed wound rotor induction machine—A comparison with alternative schemes," *IEEE Trans. Energy Convers.*, vol. 17, no. 3, pp. 414–421, Sep. 2002.
- [9] E. Muljadi, et.al., "Effect of variable speed wind turbine generator on stability of a weak grid," *IEEE Trans. Energy Convers.*, vol. 22, no. 1, pp. 29–36, Mar. 2007.
- [10] R. Pena, et.al., "Doubly fed induction generator using back-to-back PWM converters and its application to variable-speed wind-energy generation," *IEE Proc. Elect. Power Appl.*, vol. 143, no. 3, pp. 231–241, May 1996.
- [11] S. Muller, et.al., "Doubly fed induction generator systems for wind turbines," *IEEE Ind. Appl. Mag.*, vol. 8, no. 3, pp. 26–33, May/June 2002.
- [12] W. Qiao, et.al., "Grid connection requirements and solutions for DFIG wind turbines," in *Proc. IEEE Energy 2030 Conf. (ENERGY'08)*, Nov. 17–18, 2008, pp. 1–8.
- [13] A. Petersson, et.al., "Modeling and experimental verification of grid interaction of a DFIG wind turbine," *IEEE Trans. Energy Convers.*, vol. 20, no. 4, pp. 878–886, Dec. 2005.
- [14] H. M. Hasanien, et.al., "A set-membership affine projection algorithm-based adaptive-controlled SMES units for wind farms output power smoothing," *IEEE Trans. Sustain. Energy*, vol. 5, no. 4, pp. 1226–1233, Oct. 2014.
- [15] Z. Saad-Saoud, et.al., "Application of STATCOMs to wind farms," *IEE Proc. Gener. Transmiss. Distrib.*, vol. 145, no. 5, pp. 511–516, Sep. 1998.

- [16] G. O. Suvire, et.al., “Combined control of a distribution static synchronous compensator/flywheel energy storage system for wind energy applications,” *IET Gener. Transmiss. Distrib.*, vol. 6, no. 6, pp. 483–492, Jun. 2012.
- [17] D. Somayajula, et.al., “An ultra capacitor integrated power conditioner for intermittency smoothing and improving power quality of distribution grid,” *IEEE Trans. Sustain. Energy*, vol. 5, no. 4, pp. 1145– 1155, Oct. 2014.
- [18] M. T. Abolhassani, et.al., “Integrated doubly fed electric alternator/active filter (IDEA), a viable power quality solution, for wind energy conversion systems,” *IEEE Trans. Energy Convers.*, vol. 23, no. 2, pp. 642–650, Jun. 2008.
- [19] A. Gaillard, et.al., “Active filtering capability of WECS with DFIG for grid power quality improvement,” in *Proc. IEEE Int. Symp. Ind. Electron.*, Jun. 30, 2008, pp. 2365–2370.
- [20] A. Gaillard, et.al., “Reactive power compensation and active filtering capability of WECS with DFIG without any overrating,” *Wind Energy*, vol. 13, pp. 603–614, 2009.